Existence of Bistability and Correlation with Arrhythmogenesis in Paced Sheep Atria

ROBERT A. OLIVER, M.S.,*†‡ G. MARTIN HALL, PH.D.,†‡
SONYA BAHAR, PH.D.,†‡ WANDA KRASSOWSKA, PH.D.,*†‡
PATRICK D. WOLF, PH.D.,*†‡ ELLEN G. DIXON-TULLOCH, M.S.,*
and DANIEL J. GAUTHIER, PH.D.*†‡

From the Departments of *Biomedical Engineering and †Physics, and the ‡Center for Nonlinear and Complex Systems, Duke University, Durham, North Carolina

Bistability and Arrhythmogenesis in Paced Sheep Atria. *Introduction:* **Studies of the electrical dynamics of cardiac tissue are important for understanding the mechanisms of arrhythmias. This study uses high-frequency pacing to investigate the dynamics of sheep atria.**

Methods and Results: **A 504-electrode mapping plaque was affixed to the right atrium in six sheep. Cathodal pacing stimuli were delivered to the center of the plaque. Pacing period (T_p) was decreased from 275 ± 25 msec to 75 ± 25 msec and then increased to 230 ± 70 msec in steps of either 5 or 10 msec. In all 21 trials in six sheep, the atrium responded 1:1 at longer T_ps and 2:1 at shorter T_ps. As T_p was decreased, the response switched to 2:1 at a particular T_p. Conversely, as T_p was increased, the response switched back to 1:1 at a particular T_p. Over 21 trials, the 1:1-to-2:1 and 2:1-to-1:1 transitions occurred at 119.5 ± 18.8 msec and 130.0 ± 19.1 msec, respectively. This hysteretic behavior yielded bistability windows, 10.5 ± 7.2 msec wide, wherein 1:1 and 2:1 responses existed at the same T_p. In 15 trials and in all animals, idiopathic wavefronts emanating from outside the mapped region passed through the mapped region. In 13 of those trials, the idiopathic wavefronts occurred at T_ps within the bistability window or within 35 msec of its upper or lower limit.**

Conclusion: **Bistability windows and idiopathic wavefronts were observed and found to be correlated with each other, suggesting a connection between bistability and arrhythmogenesis.**
(J Cardiovasc Electrophysiol, Vol. 11, pp. 797-805, July 2000)

bistability, hysteresis, atrial arrhythmias, arrhythmogenesis, mapping, high-frequency pacing

Introduction

Studies of the electrical dynamics of cardiac tissue are important for understanding the causes and mechanisms of conduction blocks and tachyarrhythmias including atrial and ventricular fibrillation. Such understanding can augment development of effective pharmacologic and electrical cardiac therapies. One of the most revealing methods used to investigate the electrical dynamics of cardiac tissue is periodic pacing, which has been used to study experimental preparations including isolated, dissociated rabbit[1,2] and guinea pig[3] ventricular myocytes; aggregates of embryonic chick cardiac myocytes[4–8]; excised sheep Purkinje fibers[9–11]; excised canine ventricular tissue[12,13] and Purkinje fibers[14]; in vivo and excised toad ventricles[15]; right atria of excised sheep hearts[16]; and in vivo dog ventricles.[17] These studies determined the responses of the preparations to periodic pacing as a function of stimulus strength and pacing period (T_p). The observed responses included various phase-locked and irregular rhythms. One of the most important findings was the discovery that the responses sometimes exhibited period-doubling bifurcations as T_p was varied. In some cases, these bifurcations subsequently led to irregular responses. According to nonlinear dynamics theory, such bifurcations are a route to chaotic behavior.[18] Therefore, the observation of period-doubling bifurcations in the cardiac preparations described is significant because it suggests a connection between phase-locked and irregular responses on the cellular level and tachyarrhythmias on the organ level.

Although comprehensive, these studies include only one investigation of an in vivo mammalian heart.[17] Furthermore, in studies where T_p was varied, it often was

Supported in part by Grant CDR-8622201 from the National Science Foundation and by The Whitaker Foundation.

Address for correspondence: Robert A. Oliver, M.S., Department of Biomedical Engineering, Duke University, 136 Hudson Hall, Science and Research Drives, Durham, NC 27708. Fax: 919-660-5405; E-mail: robert.oliver@duke.edu

Manuscript received 22 November 1999; Accepted for publication 29 March 2000.

only decreased or increased rather than decreased then increased. This technique does not allow the investigation of two important characteristics of cardiac electrical dynamics: bistability and hysteresis. In the context of periodic pacing, bistability refers to the existence of two different phase-locked or irregular responses at the same T_p and stimulus strength. Hysteresis describes the phenomenon whereby the response undergoes a change to a different state at a different T_p when T_p is decreased than when T_p is increased.

Bistability and hysteresis as a function of stimulus strength have been observed in excised sheep Purkinje fibers and papillary muscles[19] and in isolated, dissociated guinea pig ventricular myocytes.[20] A study on frog ventricles by Mines[21] in 1913 appears to be the first documented case of the characterization of bistability and hysteresis as a function of T_p. Over 50 years later, these phenomena were reported by Moulopoulos et al.[17] in in vivo dog ventricles. Over 20 years after that, these phenomena were reported by Guevara et al. in aggregates of spontaneously beating embryonic chick cardiac myocytes[7] and isolated, dissociated rabbit ventricular myocytes[1,2] and by Hescheler and Speicher[3] in isolated, dissociated guinea pig ventricular myocytes. Hall et al.[22] extended the work of Mines by performing studies on excised frog ventricular tissue. They decremented T_p until the tissue response switched from 1:1 (1 stimulus elicits 1 beat) to 2:1 (2 stimuli elicit 1 beat). The switch occurred abruptly at a particular T_p. They then incremented T_p until the response switched back to 1:1. Again, the switch occurred abruptly at a particular T_p. The 1:1-to-2:1 transition occurred at a T_p of approximately 500 msec, whereas the 2:1-to-1:1 transition occurred at a T_p of approximately 700 msec. This hysteresis yielded a bistability window of 200 msec wherein 1:1 and 2:1 responses existed at the same T_p.

The purpose of this study was to extend the work of Hall et al. to an in vivo sheep heart. We used a cardiac mapping system to measure both temporal and spatial responses to periodic pacing. The mapping system allowed us to measure bistability and hysteresis in a spatially extended system and correlate it with arrhythmogenesis. The results of this study provide a more complete picture of the electrical dynamics of cardiac tissue and their possible connection to arrhythmogenesis.

Methods

Animal Preparations

The study was performed in accordance with a protocol that conforms to the Research Animal Use Guidelines of the American Heart Association. The protocol was approved by the Duke University Institutional Animal Care and Use Committee. Six female sheep (61 ± 2 kg) were anesthetized initially with ketamine hydrochloride 15 to 22 mg/kg intramuscularly. The surgical site was shaved, an intravenous line was established, and the animal was placed on isoflurane anesthesia administered via a nose cone. Once anesthesia was achieved, the animal was intubated with a cuffed endotracheal tube and ventilated with a ventilator (North American Drager, Telford, PA, USA). Isoflurane gas 1% to 5% was administered continuously to maintain adequate anesthesia. An orogastric tube was passed into the stomach to prevent rumen aspiration. Femoral arterial blood pressure and the lead II ECG were continuously displayed and monitored. Blood was withdrawn every 30 to 60 minutes to determine pH, pO_2, pCO_2, total CO_2, O_2 saturation, base excess, and concentrations of Ca^{2+}, K^+, Na^+, and HCO_3^-. Normal physiologic levels of these quantities were maintained by adjusting the ventilator and by intravenous infusion of electrolytes.

The chest was opened through a median sternotomy and the heart suspended in a pericardial cradle. A 3-cm × 3-cm mapping plaque was affixed to the epicardium of the right atrial free wall with sutures to the pericardial cradle and the fatty tissue in the AV groove. In some animals, a monophasic action potential (MAP) recording catheter (EP Technologies, Sunnyvale, CA, USA) was inserted into the right atrium via the right jugular vein. The MAP signals were used during the experiments to help distinguish between 1:1, 2:1, and irregular responses. MAP signals were not necessary for this study and were not used in all animals because final determination of the tissue response was based on activation animations discussed later. Finally, a defibrillation and pacing catheter (Ventritex, Sunnyvale, CA, USA) was placed in the right ventricle in some animals for emergency internal defibrillation.

Data Acquisition and Pacing

The mapping plaque contained 504 silver/silver chloride electrodes arrayed in a 21 × 24 rectangular grid with 1-mm interelectrode spacing. Monopolar extracellular electrograms were recorded from each electrode with respect to the return electrode placed in the aortic root. The electrograms were bandpass filtered from 0.5 to 500.0 Hz, sampled at 2.0 kHz, and displayed in real time on a video monitor using the mapping system described previously.[23] The mapping system recorded the electrograms on magnetic disk for later analysis. A cathodal stimulus current of 4-msec duration and ranging in strength from 0.4 to 2.0 mA was applied at the center of the plaque. The return electrode for this current was attached to the chest retractor, which remained in place during the trials. The stimulus current was generated by a constant-current source with the timing controlled by a personal computer (Tagram, Tustin, CA, USA) running custom Labview (National Instruments, Austin, TX, USA) software.

Experimental Protocol

Once the animal was fully instrumented, a normal sinus beat was recorded and analyzed to characterize signal quality and normal sinus activation of the mapped region. Next, the right atrium was paced at a constant T_p in the range from 500 to 600 msec to determine the

diastolic threshold and to confirm that a wavefront moved radially outward from the stimulus site.

It was found that the T_ps at which the 1:1-to-2:1 and 2:1-to-1:1 transitions occurred decreased with increasing current strength until reaching an asymptote corresponding to the absolute refractory period of the strength-interval relationship of cardiac tissue.[24] Therefore, the minimum current strength above which the transition T_ps no longer changed was used. Over all animals, stimulus current was between 2 and 20 times diastolic threshold.

A trial consisted of a downsweep in T_p immediately followed by an upsweep in T_p as outlined in the following. In all trials, the tissue response was 1:1 at the initial T_p of the downsweep. The downsweep consisted of the following sequence:

1. Pace at a T_p in the range of 250 to 300 msec,
2. Pace at a constant T_p for at least 3 seconds,
3. Decrease T_p by either 5 or 10 msec,
4. Repeat 2 and 3 until T_p is 100 msec or below and the tissue response is 2:1.

The upsweep consisted of the following sequence:

1. Pace at the last T_p of the downsweep,
2. Pace at a constant T_p for at least 3 seconds,
3. Increase T_p by either 5 or 10 msec,
4. Repeat 2 and 3 until T_p is 160 msec or above and the tissue response is 1:1.

At each T_p, electrograms were recorded from all electrodes for at least 2 seconds.

Data Analysis

All visualizations were performed on a Sparc 4 (Sun Microsystems, Palo Alto, CA, USA) workstation using animation software described previously.[25,26] Briefly, the electrograms from each electrode were differentiated in time using a five-point algorithm[27] and displayed as a 21×24 array of elements corresponding to the geometry of the mapping plaque. The color of each element was assigned based on the instantaneous value of the derivative of the electrogram corresponding to that element. Animations of the array showed propagating wavefronts, thereby characterizing the spatial and temporal responses of the tissue under the plaque. Such animations were viewed during and after the trials.

Animations of all T_ps from all trials were viewed and the response at each T_p was classified as 1:1, 2:1, idiopathic wavefronts (defined later), or some combination thereof. A 1:1 response was characterized as a wavefront moving radially outward from the stimulus site following each stimulus. A 2:1 response was characterized as such a wavefront following every other stimulus. Idiopathic wavefronts were characterized as those that did not originate at the stimulus site and were not synchronized with the stimuli. The idiopathic wavefronts were classified further as single wavefront, multiple wavefronts, and rotor-like. As illustrated later, rotor-like describes wavefronts whose directions of propagation rotated as they crossed the mapped region.

A computer program was used to determine activation times at all plaque electrodes. For a given activation event, the time of the steepest negative deflection of the corresponding activation complex is considered to be the activation time of that event.[28] All electrograms were reviewed and the activation times were edited manually.

The original activation times contained spatial noise that interfered with creating accurate activation maps and estimating conduction velocities. Therefore, they were spatially filtered using SAS/GRAPH (SAS Institute, Cary, NC, USA).[29] The SAS/GRAPH procedure G3GRID was used with bivariate splines and smoothing values of 0.8 or 0.9. These smoothing values were chosen so that procedure GCONTOUR created smooth activation maps in Figures 1, 2, and 3 that were close to the animations described earlier.

The G3GRID-generated activation times were input to a computer program that estimated conduction velocities at all interior electrodes based on the activation times at the electrode and its eight closest neighbors. The program assumed that a plane wave traveled across the nine-electrode group and determined its velocity by least-squares fitting. For paced beats, the velocities at electrodes within 4 mm of the stimulus site were not estimated because accurate activation times could not be determined due to the stimulus artifacts. The mean and SD of all calculated velocities across the plaque were determined for normal sinus beats and paced beats. All comparisons of conduction velocities were made using paired-difference *t*-tests.

Results

Normal Sinus Beat and Paced Beat

Figure 1 shows differentiated electrograms and activation maps for a normal sinus beat with an interbeat interval of 695 msec (panel A) and a paced beat during pacing with a T_p of 600 msec (panel B). Both were taken from animal 1. The electrograms shown in panels A and B were chosen from different sites to help ensure that all regions of the plaque were shown at least once across Figures 1, 2, and 3. As expected, the activation front of the normal sinus beat entered at the top of the plaque, consistent with activation of the sinoatrial node, and then moved toward the bottom of the plaque near the AV groove. The map shows no locations of conduction block and only slight inhomogeneity. As expected, the activation front of the paced beat was initiated at the stimulus site and moved radially outward off the plaque. The map shows no locations of conduction block and only mild anisotropy as exhibited by a slightly elliptical activation pattern. The mean conduction velocities of the normal sinus beat and the paced beat were 102.9 ± 27.5 cm/sec and 94.7 ± 17.2 cm/sec, respectively.

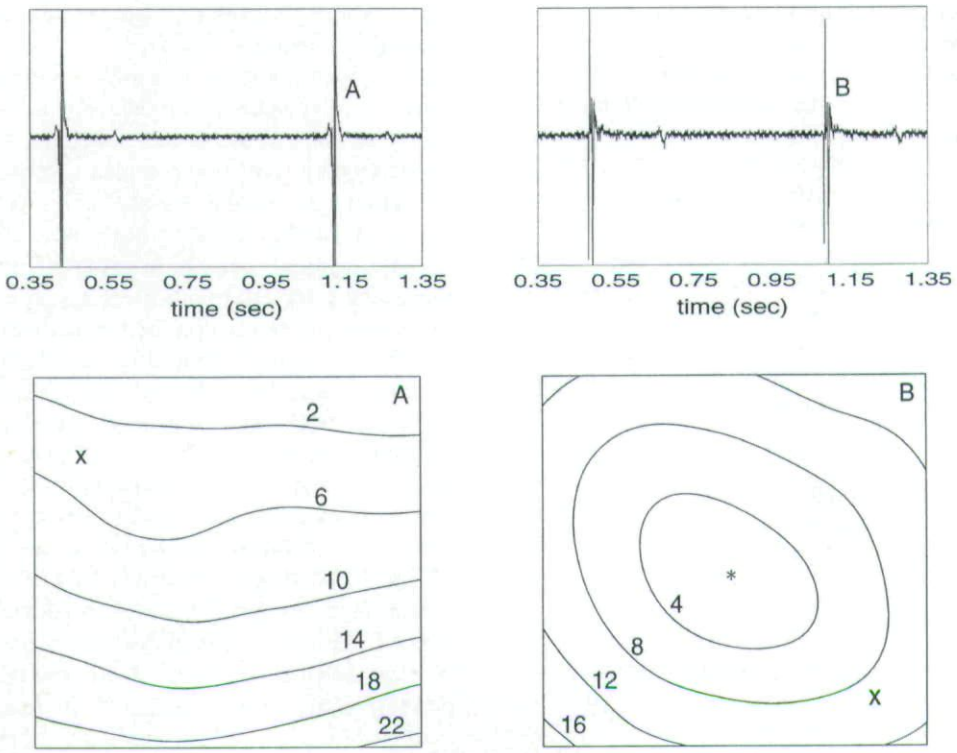

Figure 1. *Differentiated electrograms and activation maps for a normal sinus beat (A) and a paced beat (B). Each location of the electrodes at which the electrograms in the upper panels were recorded is marked on the activation maps with an "x." The activation complexes shown in the maps are marked on the electrograms with an "A" or "B," as appropriate. (A) Normal sinus beat. Activation isochrones are in milliseconds, measured with respect to the first activation detected under the plaque. (B) Beat following stimulation at the center of the plaque with T_p = 600 msec. The response was 1:1 during pacing. The stimulus site is marked on the activation map with an asterisk. Stimulus artifacts appear as negative spikes immediately followed by positive spikes whose combined amplitudes nearly span the vertical height of the electrogram. Activation isochrones are in milliseconds, measured from the beginning of each stimulus.*

1:1 Response and 2:1 Response

Figure 2 shows differentiated electrograms and activation maps for 1:1 and 2:1 responses during the same trial in animal 1. The stimulus strength was kept constant during the downsweep and the upsweep of the trial. The activation maps of panels A and B are for pacing at 120 msec on the downsweep; the activation map of panel C is for pacing at 120 msec on the upsweep. Despite being paced at the same T_p, the responses were different.

A 1:1 response was characterized by activations following each stimulus that led to propagating wavefronts that moved radially outward from the stimulus site. As noted on the differentiated electrogram, the activation maps of panels A and B show successive beats and therefore demonstrate a 1:1 response. They show activation patterns similar to each other and to that of the paced beat of Figure 1. The mean conduction velocities were 63.0 ± 21.5 cm/sec (panel A) and 60.6 ± 13.5 cm/sec (panel B). These velocities were comparable to each other ($P = 0.036$). Furthermore, these velocities that occurred when T_p was 120 msec were significantly less ($P < 0.0005$) than the velocity of the paced beat of Figure 1, which occurred when T_p was 600 msec. A reduction in conduction velocity following a reduction in T_p and therefore diastolic interval is consistent with the conduction-velocity restitution property of cardiac tissue.[30]

A 2:1 response was characterized by activations following every other stimulus that led to propagating wavefronts that moved radially outward from the stimulus site. The differentiated electrogram corresponding to the activation map of panel C shows activation complexes after every other stimulus and therefore demonstrates a 2:1 response. The activation pattern in panel C is similar in shape to the 1:1 beats of panels A and B and to that of the paced beat of Figure 1. The mean conduction velocity of 90.3 ± 17.1 cm/sec that occurred when T_p was 120 msec was significantly greater than ($P < 0.0005$) the velocity of the 1:1 beats, which also occurred when T_p was 120 msec but was significantly less than ($P < 0.0005$) the velocity of the paced beat of Figure 1, which occurred when T_p was 600 msec.

During the analysis of these trials and all other trials in animal 1, electrograms from the center and each of the corners of the mapped region were analyzed with each animation. In all other animals, typically two or more electrograms from different positions were viewed. In all cases, the responses were the same in each electrogram and the animation, suggesting the entire mapped region behaved consistently. In no cases did one area respond

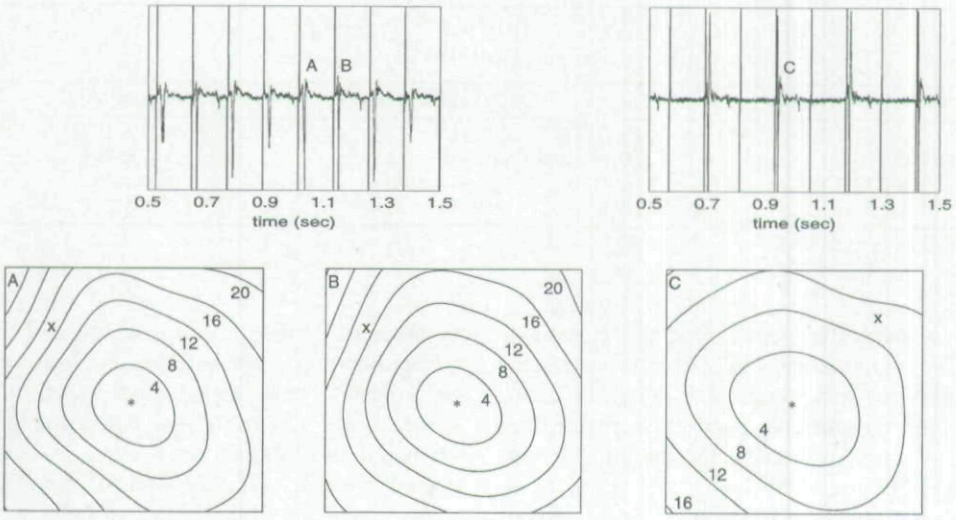

Figure 2. *Differentiated electrograms and activation maps for 1:1 and 2:1 responses with T_p = 120 msec. Each location of the electrodes at which the electrograms in the upper panels were recorded is marked on the activation maps with an "x." The stimulus site is marked on the activation maps with an asterisk. The activation complexes shown in the maps are marked on the electrograms with an "A," "B," or "C," as appropriate. Stimulus artifacts appear as negative spikes immediately followed by positive spikes whose combined amplitudes span the vertical height of the electrograms. Activation isochrones are in milliseconds, measured from the beginning of each stimulus. (A, B) 1:1 response, T_p = 120 msec on the downsweep. Successive paced beats. (C) 2:1 response, T_p = 120 msec on the upsweep.*

1:1 while another responded 2:1. If such a heterogeneous response occurred, it was either highly transient or occurred outside the mapped region.

Bistability

The bistability illustrated in Figure 2 was present in 17 of 19 trials in 5 of 6 sheep, as summarized in Table 1. Because T_p was changed in discrete steps, it was impossible to determine the exact transitions. Therefore, the 1:1-to-2:1 transition was taken as the T_p at which 2:1 first occurred plus one half the step size. Likewise, the 2:1-to-1:1 transition was taken as the T_p at which the response reverted to 1:1 minus one half the step size. In all cases of bistability, the 1:1-to-2:1 transition occurred at a shorter T_p than the 2:1-to-1:1 transition which resulted in hysteresis in the responses. In 2 of the 19 trials in animals 1 through 5 and in two trials in animal 6, the 1:1-to-2:1 and 2:1-to-1:1 transitions occurred at the same T_ps. However, it is important to note that bistability windows narrower than 5 or 10 msec could not be detected because T_p was changed in discrete steps of 5 or 10 msec.

Table 2 lists mean conduction velocities during 1:1 and 2:1 responses in animals 1, 2, 3, and 5. For each animal, the velocities listed are for the same T_p in the same trial, with the 1:1 beat occurring on the downsweep and the 2:1 beat occurring on the upsweep. In all cases, the 2:1 velocity is significantly greater than the 1:1 velocity ($P < 0.0005$). No data are listed for animal 4 because there were no trials that had 1:1 and 2:1 responses at the same T_p due to the presence of idiopathic wavefronts. Nothing is listed for animal 6 due to the absence of bistability windows within the experimental detection sensitivity.

Idiopathic Wavefronts

In 15 trials, the tissue was not captured by the stimuli at T_ps within and near the bistability window. Rather, wavefronts from outside the mapped region were seen to

TABLE 1

Measured Response Transition T_ps and Bistability Windows

Animal	Total Trials	1:1-to-2:1 (msec)	2:1-to-1:1 (msec)	Window (msec)
1	5	110.0 (102.5–125.0)	118.0 (112.5–125.0)	08.0 (00.0–15.0)
2	2	122.5 (112.5–132.5)	147.5 (137.5–157.5)	25.0 (25.0–25.0)
3	2	106.3 (105.0–107.5)	113.8 (112.5–115.0)	07.5 (05.0–10.0)
4	5	102.0 (095.0–105.0)	112.0 (105.0–115.0)	10.0 (10.0–10.0)
5	5	137.5 (127.5–142.5)	150.5 (147.5–157.5)	13.0 (10.0–20.0)
6	2	152.5 (142.5–162.5)	152.5 (142.5–162.5)	00.0 (00.0–0.00)
All trials	21	119.5 (095.0–162.5)	130.0 (105.0–162.5)	10.5 (00.0–25.0)

Values are given as mean (range).

TABLE 2
Conduction Velocities During 1:1 and 2:1 Responses

Animal	Bistability Window	T_p	1:1 Velocity (cm/sec)	2:1 Velocity (cm/sec)	P Value
1	107.5–122.5	120.0	63.0 ± 21.5	90.3 ± 17.1	<0.0005
2	112.5–137.5	125.0	80.3 ± 18.8	99.2 ± 28.8	<0.0005
3	107.5–112.5	110.0	66.6 ± 16.7	86.6 ± 18.7	<0.0005
5	127.5–147.5	145.0	70.7 ± 20.8	91.4 ± 27.0	<0.0005

Velocity values are given as mean ± SD.

invade the region under the plaque. Due to the limited size of the mapped region, it was impossible to determine the type of underlying arrhythmia associated with the wavefronts. In one instance, the pacing terminated the wavefronts; in all other instances, the pacing had no effect on the wavefronts in the mapped region. It is unclear if the pacing had any effect outside the mapped region.

For the purpose of this article, these wavefronts are called idiopathic wavefronts. Figure 3 shows activation maps for the most commonly observed types of idiopathic wavefronts. Panel A shows a wavefront that originated inferior to the plaque and propagated superiorly across the mapped region. Similar wavefronts moved across the mapped region in many directions even in the same animal during the same trial. Panel B shows two wavefronts moving toward each other. Such wavefronts interacted in a number of ways, including colliding then annihilating and colliding then merging. Panel C shows a rotor-like wavefront whose direction of propagation rotated as the wavefront crossed the mapped region.

Based on visual examination, the differentiated electrograms of Figure 3 differ from those of Figure 2 in that the activation complexes are less periodic, vary more from beat to beat, and are not synchronized with the stimuli. In some trials, the activation patterns of the idiopathic wavefronts were even less organized than described earlier. The duration of the idiopathic wavefronts varied from 1 to 10 beats. Finally, even at the same T_p, the response often changed quickly, going from different types of idiopathic wavefronts to paced beats and many combinations thereof.

Table 3 shows that idiopathic wavefronts occurred in 15 of the 21 total trials and in all six animals. In four animals these wavefronts occurred in every trial, whereas in two animals they did not occur in every trial. Figure 4 shows the relationship between the T_ps at which idiopathic wavefronts occurred and the bistability windows. In all 13 trials in animals 1 through 5, these wavefronts occurred at T_ps within the bistability window or within 35 msec of its upper or lower limit. The same is true for the two trials in animal 6, with the exception of the idiopathic wavefronts that occurred at much shorter T_ps than the bistability window, between 75 and 85 msec.

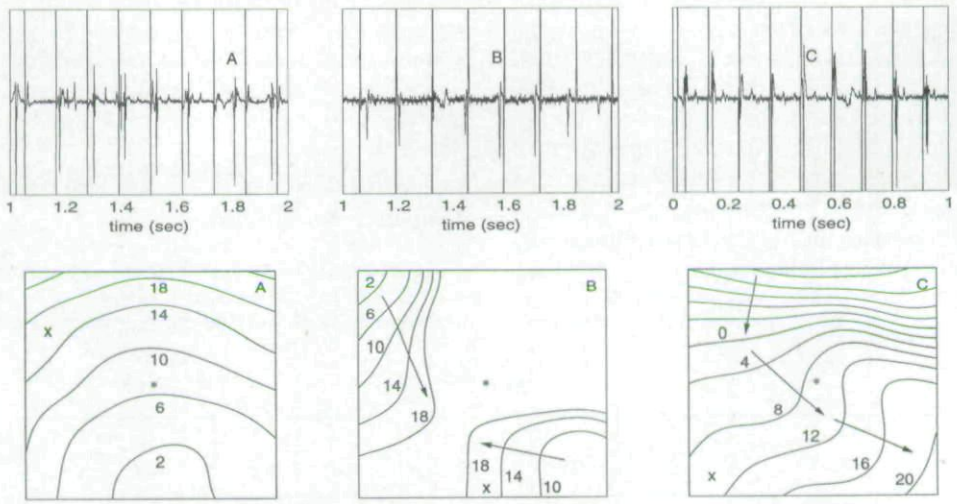

Figure 3. *Differentiated electrograms and activation maps for idiopathic wavefronts with T_p = 115, 130, and 110 msec. Each location of the electrodes at which the electrograms in the upper panels were recorded is marked on the activation maps with an "x." The stimulus site is marked on the activation maps with an asterisk. The activation complexes shown in the maps are marked on the electrograms with an "A," "B," or "C," as appropriate. The stimulus artifacts appearing as negative spikes immediately followed by positive spikes whose combined amplitudes span the vertical height of the electrograms confirm the tissue was continuously paced. (A) Single wavefront, T_p = 115 msec, animal 2. Activation isochrones are in milliseconds, measured with respect to the first activation detected under the plaque. (B) Multiple wavefronts, T_p = 130 msec, animal 4. Activation isochrones are in milliseconds, measured with respect to the first activation detected under the plaque. (C) Rotor-like wavefront, T_p = 110 msec, animal 3. Activation isochrones are in milliseconds, measured from the beginning of the stimulus.*

TABLE 3
Prevalence and Types of Idiopathic Wavefronts

Animal	Total Trials	Idiopathic*	Single Wave†	Multiple Waves†	Rotor-Like†
1	5	3	2	1	0
2	2	2	2	1	0
3	2	2	2	2	1
4	5	5	5	5	3
5	5	1	1	1	0
6	2	2	2	0	0
All trials	21	15	14	10	4

* Number of trials in which one or more types of idiopathic wavefronts were observed.
† Number of trials in which the specified type of idiopathic wavefront was observed.

These wavefronts were correlated with a 2:1-to-3:1 transition that occurred at 70 msec. Finally, although not obvious from the pooled representation of Figure 4, in all trials 2:1 responses occurred at T_ps shorter than those at which idiopathic wavefronts occurred.

Discussion

Bistability

Figure 4 and Table 1 clearly demonstrate the existence of hysteresis and bistability between the 1:1 and 2:1 responses in paced sheep atria. The response transition T_ps and the widths of the bistability windows varied only slightly from trial to trial in the same animal and only moderately among animals. To our knowledge, this is the first time such behavior has been documented in vivo in a sheep heart.

Hysteresis and bistability can be explained qualitatively by considering the action potential duration (APD) restitution property that relates APD to the preceding diastolic interval (DI). In the context of pacing, DI equals T_p minus APD. In general, APD decreases as DI decreases.[30] During the downsweep, T_p decreases so DI and APD decrease. Eventually, a stimulus comes too early in the refractory period to elicit an action potential and the tissue response switches to 2:1. The effective T_p is suddenly doubled, so DI and APD suddenly increase. As the downsweep continues, T_p, DI, and APD again decrease. After the downsweep ends, the upsweep begins and T_p, DI, and APD increase. On reaching the 1:1-to-2:1 transition, the response does not revert to 1:1 because T_p is effectively doubled and therefore DI and APD are longer than they were on the downsweep. Because the APD is longer, every other stimulus comes too early in the refractory period to elicit an action potential and a 2:1 response continues. As the upsweep continues, T_p, DI, and APD increase until every stimulus comes sufficiently late to elicit an action potential and the response reverts to 1:1. Because the T_p of the 2:1-to-1:1 transition is longer than the T_p of the 1:1-to-2:1 transition, a window of bistability results wherein 1:1 and 2:1 responses exist at the same T_ps.

Hall et al.[22] used a similar pacing protocol on excised frog ventricular tissue and found bistability in 74% of animals. The results of the present study were qualitatively similar to but quantitatively different than those of

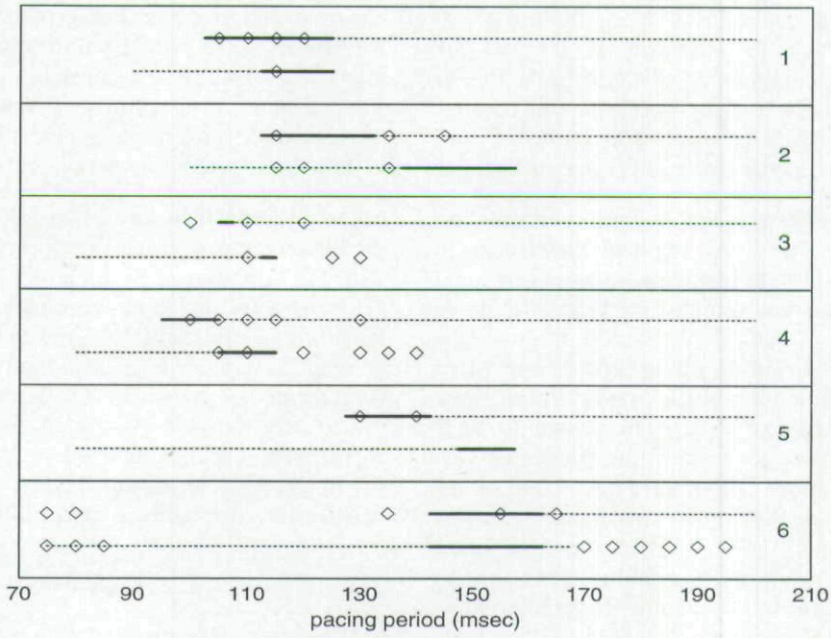

Figure 4. *Responses and idiopathic wavefronts in six animals. For each animal (numbers on the right) over all trials: (1) the two solid horizontal lines show the range of T_ps where the 1:1-to-2:1 (upper line) and the 2:1-to-1:1 (lower line) transitions occurred, and (2) the two dotted horizontal lines show the range of T_ps where the response was 1:1 (upper line) and 2:1 (lower line). Diamonds show T_ps at which idiopathic wavefronts occurred.*

their study. Specifically, the 1:1-to-2:1 transition occurred at approximately 120 msec in sheep versus 500 msec in frogs, and the 2:1-to-1:1 transition occurred at approximately 130 msec in sheep versus 700 msec in frogs. Furthermore, the width of the bistability windows was approximately 10 msec in sheep versus 200 msec in frogs. Such differences are consistent with species-specific normal sinus interbeat interval and APD. Specifically, in these studies, the normal sinus interbeat interval was approximately 700 msec in sheep and 1,000 msec in frogs, whereas APD was approximately 160 msec in sheep and 700 msec in frogs. Despite quantitative differences, the existence of bistability in small pieces of excised amphibian ventricular tissue and in in vivo mammalian atria suggests that rate-dependent bistability is a characteristic common to all cardiac tissue. This conclusion is supported further by the documentation of bistability in the literature referred to earlier.

Idiopathic Wavefronts, Conduction Velocity, Alternans, and Arrhythmias

A second intriguing result is the appearance of idiopathic wavefronts and their correlation with the bistability windows. The types of idiopathic wavefronts seen in this study and illustrated in Figure 3 are similar to those seen in fibrillation[31] and other tachyarrhythmias. The results of this study suggest that transitions between 1:1 and 2:1 responses and the corresponding bistability window constitute a marker for vulnerability to arrhythmogenesis. Knowing the bistability window or at least one of the transition T_ps would appear to predict the T_ps at which cardiac tissue is susceptible to the development of tachyarrhythmias that could lead to fibrillation.

Table 2 shows that the bistability in 1:1 and 2:1 responses extends to conduction velocity as well. Due to its effect on activation wavelength, conduction velocity is thought to play a role in atrial arrhythmias[32,33] and therefore could have played a role in the maintenance of the idiopathic wavefronts. Furthermore, heterogeneity of electrophysiologic properties is thought to contribute to arrhythmogenesis.[33] Therefore, regional differences in tissue response (1:1 or 2:1) with corresponding regional differences in conduction velocity might contribute to arrhythmogenesis.

In the literature, period-doubling bifurcations often are associated with vulnerability to fibrillation. Period-doubling bifurcations have been shown to be a route to irregular behavior in periodic pacing of various cardiac preparations and in unidimensional return maps of models and various experimental cardiac preparations.[3–5,7–9,11,12,14,15,34,35] A 2:2 response, often called alternans, is when each stimulus elicits a beat but the beats alternate in one or more characteristics. Transition from a 1:1 response to a 2:2 response is an example of a period-doubling bifurcation.

Often, transmembrane potential is measured and APD or action potential amplitude is investigated as a dynamic variable. In this context, alternans describes the situation where the elicited action potentials alternate in duration or amplitude. The APD versus T_p bifurcation diagrams from the study of frogs by Hall et al.[22] show that alternans occurred 35% of the time and was always followed by a transition to 2:1. APD could not be measured in our study because extracellular signals give no direct information on repolarization in the atria. Therefore, it was not possible to determine if alternans occurred before the onset of idiopathic wavefronts. In future studies, transmembrane potential should be measured and APD should be investigated through more extensive use of MAP electrodes. Alternatively, extracellular electrograms could be analyzed for indirect measurement of APD alternans. However, doing so might be complicated by ventricular excitation signals that sometimes appear in extracellular atrial measurements. Therefore, controlling the timing of ventricular activity would be required.

Another limitation of the study was that only a portion of the atrium was mapped due to the size of the mapping plaque. Therefore, it was impossible to know how the tissue behaved away from the plaque and whether reentrant loops or ectopic foci were present. Furthermore, data were taken for only 2 seconds at each T_p, making it difficult to capture transitions from 1:1 or 2:1 to idiopathic wavefronts. Lack of such information made it difficult to identify the origin and the conditions required for maintenance of idiopathic wavefronts. In future studies, a mapping plaque covering a larger portion of the atrium should be used and data should be taken for a longer time.

An interesting question not answered by this study is whether the idiopathic wavefronts could become sustained tachyarrhythmias. In this study, the pacing protocols were completed even if idiopathic wavefronts occurred. Interrupting the protocols when idiopathic wavefronts occur would help provide insights. For example, T_p could be held constant or the pacing could be stopped and the response monitored to determine how the idiopathic wavefronts evolved.

Finally, as previously noted, the idiopathic wavefronts disappeared and were replaced with 2:1 responses as T_p became shorter than the 1:1-to-2:1 transition. Likewise, the idiopathic wavefronts disappeared and were replaced with 1:1 responses as T_p became longer than the 2:1-to-1:1 transition. Idiopathic wavefronts appear to be correlated with these transitions and may be capable of becoming sustained tachyarrhythmias. Because pacing decremented or incremented to T_ps shorter or longer than these transitions led to disappearance of the idiopathic wavefronts, pacing delivered at the onset of tachyarrhythmias may terminate them. Overdrive pacing has been observed to convert atrial flutter in humans.[36,37]

Conclusion

This study demonstrated the existence of hysteresis in the response of in vivo sheep hearts to high-frequency pacing. The resulting bistability between 1:1 and 2:1 responses was correlated with the appearance of idiopathic wavefronts suggesting a connection between

bistability and arrhythmogenesis. The details of that connection and the causes and mechanisms of the idiopathic wavefronts remain unknown and require further study.

References

1. Guevara MR, Alonso F, Jeandupeux D, Ginneken ACGV: Alternans in periodically stimulated isolated ventricular myocytes: experiment and model. In Goldbeter A, ed: *Cell to Cell Signalling: From Experiments to Theoretical Models.* Academic Press Limited, London, 1989, pp. 551–563.
2. Yehia AR, Jeandupeux D, Alonso F, Guevara MR: Hysteresis and bistability in the direct transition from 1:1 to 2:1 rhythm in periodically driven single ventricular cells. Chaos 1999;9:916–931.
3. Hescheler J, Speicher R: Regular and chaotic behaviour of cardiac cells stimulated at frequencies between 2 and 20 Hz. Eur Biophy J 1989;17:273–280.
4. Guevara MR, Glass L, Shrier A: Phase locking, period-doubling bifurcations, and irregular dynamics in periodically stimulated cardiac cells. Science 1981;214:1350–1353.
5. Glass L, Guevara MR, Shrier A, Perez R: Bifurcation and chaos in a periodically stimulated cardiac oscillator. Physica 1983;7D:89–101.
6. Guevara MR, Ward G, Shrier A, Glass L: Electrical alternans and period-doubling bifurcations. In: *Computers in Cardiology.* IEEE Computer Society, Silver Spring, MD, 1984, pp. 167–170.
7. Guevara MR, Shrier A, Glass L: Chaotic and complex cardiac rhythms. In Zipes DP, Jalife J, eds: *Cardiac Electrophysiology: From Cell to Bedside.* WB Saunders, Philadelphia, 1990, pp. 192–201.
8. Kowtha VC, Kunysz A, Clay JR, Glass L, Shrier A: Ionic mechanisms and nonlinear dynamics of embryonic chick heart cell aggregates. Prog Biophys Mol Biol 1994;61:255–281.
9. Chialvo DR, Jalife J: Non-linear dynamics of cardiac excitation and impulse propagation. Nature 1987;330:749–752.
10. Chialvo DR, Jalife J: On the non-linear equilibrium of the heart: Locking behavior and chaos in Purkinje fibers. In Zipes DP, Jalife J, eds: *Cardiac Electrophysiology: From Cell to Bedside.* WB Saunders, Philadelphia, 1990, pp. 201–214.
11. Chialvo DR, Gilmour RF Jr, Jalife J: Low dimensional chaos in cardiac tissue. Nature 1990;343:653–657.
12. Watanabe M, Otani NF, Gilmour RF Jr: Biphasic restitution of action potential duration and complex dynamics in ventricular myocardium. Circ Res 1995;76:915–921.
13. Karagueuzian HS, Khan SS, Hong K, Kobayashi Y, Denton T, Mandel WJ, Diamond GA: Action potential alternans and irregular dynamics in quinidine-intoxicated ventricular muscle cells: Implications for ventricular proarrhythmia. Circulation 1993;87:1661–1672.
14. Gilmour RF Jr, Otani NF, Watanabe MA: Memory and complex dynamics in cardiac Purkinje fibers. Am J Physiol 1997;272: H1826–H1832.
15. Savino GV, Romanelli L, Gonzalez DL, Piro O, Valentinuzzi ME: Evidence for chaotic behavior in driven ventricles. Biophys J 1989;56:273–280.
16. Gray RA, Pertsov AM, Jalife J: Incomplete reentry and epicardial breakthrough patterns during atrial fibrillation in the sheep heart. Circulation 1996;94:2649–2661.
17. Moulopoulos SD, Kardaras N, Sideris DA: Stimulus-response relationship in dog ventricle in vivo. Am J Physiol 1965;208:154–157.
18. Strogatz SH: *Nonlinear Dynamics and Chaos. With Applications to Physics, Biology, Chemistry, and Engineering.* Addison-Wesley, Reading, PA, 1994, pp. 348–387.
19. Lorente P, Davidenko J: Hysteresis phenomena in excitable cardiac tissues. An N Y Acad Sci 1990;591:109–127.
20. Lorente P, Delgado C, Delmar M, Henzel D, Jalife J: Hysteresis in excitability of isolated guinea pig ventricular myocytes. Circ Res 1991;69:1301–1315.
21. Mines GR: On dynamic equilibrium in the heart. J Physiol 1913; 46:349–383.
22. Hall GM, Bahar S, Gauthier DJ: Prevalence of rate-dependent behaviors in cardiac muscle. Phys Rev Lett 1999;82:2995–2998.
23. Wolf PD, Rollins DL, Blitchington TF, Ideker RE, Smith WM: Design for a 512 channel cardiac mapping system. In Mikulecky DC, Clarke AM, eds: *Biomedical Engineering: Opening New Doors. Proceedings of the Fall 1990 Annual Meeting of the Biomedical Engineering Society.* New York University Press, New York, 1990, pp. 5–13.
24. Alferness C, Bayly PV, Krassowska W, Daubert JP, Smith WM, Ideker RE: Strength-interval curves in canine myocardium at very short cycle lengths. PACE 1994;17:876–881.
25. Laxer C, Ideker RE, Smith WM, Wolf PD, Simpson EV: A graphical display system for animating mapped cardiac potentials. In: *Proceedings of the 3rd IEEE Symposium on Computer-Based Medical Systems.* 1990, pp. 197–204.
26. Laxer C, Alferness CA, Smith WM, Ideker RE: The use of computer animation of mapped cardiac potentials in studying electrical conduction properties of arrhythmias. In Murray A, Arzbaecher R, eds: *Proceedings Computers in Cardiology.* IEEE Computer Sciences Press, Los Alamitos, CA, 1991, pp. 23–26.
27. Burden RL, Faires JD, Reynolds AC: *Numerical Analysis.* Prindle, Weber, and Schmidt, Boston, 1978, p. 177.
28. Spach MS, Kootsey JM: Relating the sodium current and conductance to the shape of transmembrane and extracellular potentials by simulation: Effects of propagation boundaries. IEEE Trans Biomed Eng 1985;BME-32:743–755.
29. *SAS/GRAPH User's Guide, Release 6.03 Edition.* SAS Institute Inc., Cary, NC, 1988, pp. 479–488.
30. Boyett MR, Jewell BR: Analysis of the effects of changes in rate and rhythm upon electrical activity in the heart. Prog Biophys Mol Biol 1980;36:1–52.
31. Konings KTS, Kirchhof CJHJ, Smeets JRLM, Wellens HJJ, Penn OC, Allessie MA: High-density mapping of electrically induced atrial fibrillation in humans. Circulation 1994;89:1665–1680.
32. Allessie MA, Bonke FIM: Atrial arrhythmias: Basic concepts. In Mandel WJ, ed: *Cardiac Arrhythmias.* Third Edition. JB Lippincott, Philadelphia, 1995, pp. 297–326.
33. Allessie MA: Reentrant mechanisms underlying atrial fibrillation. In Zipes DP, Jalife J, eds: *Cardiac Electrophysiology: From Cell to Bedside.* Second Edition. WB Saunders, Philadelphia, 1995, pp. 562–566.
34. Guevara MR, Glass L: Phase locking, period doubling bifurcations and chaos in a mathematical model of a periodically driven oscillator: A theory for the entrainment of biological oscillators and the generation of cardiac dysrhythmias. J Math Biol 1982;14:1–23.
35. Glass L, Zeng W: Complex bifurcations and chaos in simple theoretical models of cardiac oscillators. Ann N Y Acad Sci 1990;591:316–327.
36. Waldo AL: Atrial flutter: mechanisms, clinical features, and management. In Zipes DP, Jalife J, eds: *Cardiac Electrophysiology: From Cell to Bedside.* Second Edition. WB Saunders, Philadelphia, 1995, pp. 666–681.
37. Shenasa H, Curry PVL, Shenasa M: Atrial arrhythmias: clinical concepts and advances in mechanism and management. In Mandel WJ, ed: *Cardiac Arrhythmias.* Third Edition. JB Lippincott, Philadelphia, 1995, pp. 327–367.